Nonlinear Dyn (2012) 67:2063–2080
DOI 10.1007/s11071-011-0129-9

ORIGINAL PAPER

Data-based Identification of nonlinear restoring force under spatially incomplete excitations with power series polynomial model

Bin Xu · Jia He · Sami F. Masri

Received: 13 June 2010 / Accepted: 8 June 2011 / Published online: 16 July 2011

Abstract One of the present barriers to the realization of structural health monitoring is the lack of efficient and general identification methodologies for dealing with nonlinearity, because a priori knowledge of the nature and mathematical form of the nonlinearities of typical engineering structures are usually unknown. The studies on the identification of restoring force, which can be considered as a direct indicator of the extent of the nonlinearity, have received increasing attention in recent years. In this paper, the nonlinear restoring force (NRF) was estimated by using a power series polynomial, and each coefficient of the polynomial was identified by means of standard least-square techniques. No information about the system was needed, and only the applied excitations and the corresponding response time series were used for the identification. Two different cases, in which the system was under complete and incomplete excitations, were investigated. Moreover, the effect of noise level was also taken into consideration. The feasibility and robustness of the proposed approach were verified via a 2-degree-of-freedom (DOF) lumped-mass numerical model, and experimental tests on a 4-story shear building with magneto-rheological (MR) dampers which served to simulate nonlinear behavior. The results show that the proposed data-based method is capable of identifying the NRF in a chain-like multi-degree-of-freedom engineering structures without any assumptions on the structural parameters, and provides a promising way for damage detection in the presence of structural nonlinearities.

Keywords Nonlinear restoring force · System identification · Complete and incomplete inputs · Time series · MR dampers · Least-square techniques · Noise

B. Xu (✉) · J. He · S.F. Masri
College of Civil Engineering, Hunan University, Changsha, 410082 Hunan, China
e-mail: binxu@hnu.edu.cn

B. Xu
Key Laboratory of Building Safety and Energy Efficiency (Hunan University), Ministry of Education, Changsha, 410082 Hunan, China

S.F. Masri
Department of Civil Engineering, University of Southern California, Los Angeles, CA 90089, USA

1 Introduction

Due to the rapid increase in the number of damaged or deteriorated structures, it is crucial to evaluate their current reliability, performance, and condition for the prevention of potentially catastrophic events, as well as for remaining life estimation. An investigation reported by Ghanem and Shinozuka [3] reviewed the application of a number of system identification techniques in earthquake engineering. Furthermore, Doebling et al. [2] and Wu et al. [29] presented a recent thorough review of vibration-based

damage identification methods. Most of the currently available vibration-based model updating and identification methods for structural damage detection are based on the idea of extracting the eigenvalues, mode shapes, and mode shape derivatives from the dynamic responses, and strictly speaking are only suitable for linear systems. However, nonlinearities exist widely in engineering structures, as the occurrence of a fault in an initially linear structure will, in many cases, result in nonlinear behavior. All engineering structures are nonlinear to some extent, and the nonlinearity is caused by one or a combination of several factors such as crack initiation and development, and the looseness and presence of friction characteristics of structural joints. Therefore, the detection of nonlinearities is receiving increased attention and considered of high importance for diagnosis of faults in structures.

The field of nonlinear structural dynamics has been studied for a relatively long time, but the first contribution to the identification of nonlinear structural models can be traced back to the 1970s [5]. Since then, numerous methods have been developed due to the highly individualistic nature of nonlinear systems [8]. Using information about the state variables of nonlinear systems, Masri and Caughey [9] proposed a fruitful approach, named the restoring force surface (RFS) method, to identify and express the nonlinear system characteristics in terms of orthogonal functions, e.g. Chebyshev polynomial. The RFS method was first developed for a wide class of single-degree-of-freedom (SDOF) dynamic system, but the study on the generalization to multi-degree-of-freedom (MDOF) systems soon followed [10]. The method was extremely appealing in its simplicity because its starting point was Newton's second law. Masri et al. [11, 12] developed a self-starting, multi-stage, time-domain approach for the nonparametric identification of nonlinear MDOF systems undergoing free oscillations or subjected to arbitrary direct force excitations and/or non-uniform support motions. Worden and Tomlinson [28] described numerous approaches for the detection, identification, and modeling of nonlinear systems in their textbook. Based on the uses of power series expansions, a relatively simple nonparametric technique for the identification of nonlinearities of a variety of discrete nonlinear vibrating systems has been developed by Yang and Ibrahim [24]. Kerschen et al. [7] proposed an algorithm based on a Bayesian inference approach for the screening of nonlinear system models. Based on the applied excitation(s) and resulting acceleration, a general procedure was presented for the direct identification of the state equation of complex nonlinear system [13]. In the following years, Masri et al. [14, 15] extended their work to present a general data-based approach by using power series fitting techniques for developing reduced-order, nonparametric models in nonlinear MDOF systems. More recently, Tasbihgoo et al. [17] discussed two broad classes of methods. One class relied on the representation of the system restoring forces in a polynomial-basis format while the other used artificial neural networks to map the complex transformations for developing nonparametric models of nonlinear MDOF systems. In the works by Yun et al. [25], model-free identification techniques utilizing nonparametric system identification approaches were used to detect the changes of the nonlinear system, to interpret the physical meaning of the detected changes, and to quantify the uncertainty of the detected system changes.

In most of the approaches above, all excitations (inputs) applied to the nonlinear structural system should be known and available for the nonlinearity identification. But in practice it is either too difficult to excite all of the DOFs of a structure for identification, or part of the dynamic response measurements and the external excitations of the structure are unavailable due to inaccessibility and the limitation of the number of available sensors. To handle this problem, great efforts have been made in this area by many investigators during recent years. Mohammad et al. [16] proposed a direct parameter estimation method for identifying the physical parameters of linear and nonlinear MDOF structures with only one input excitation. Using a recursive least-squares estimation with unknown inputs (RLSE-UI) approach and Extended Kalman filter (EKF), Yang et al. [21–23] identified the parameters of a nonlinear structure as well as the unmeasured excitations. For local-level system identification, a finite-element-based procedure was used to identify the stiffness and damping coefficients of the system without inputs [6, 26, 27]. More recently, based on the basic idea of equivalent linearization and the symmetry of the identified stiffness matrix, Xu et al. [20] proposed a data-based model-free hysteresis identification approach for nonlinear systems under incomplete excitations.

In this paper a power series polynomial modeling approach involving the instantaneous values of the state variables of the system was proposed to repre-

sent the system nonlinearities. Based on the excitations and the corresponding response time series, each coefficient of the polynomial was identified by means of standard least-square techniques without any assumptions and prior knowledge of the system. Two different cases, in which the system was under complete and incomplete excitations, were investigated. The feasibility and robustness of the proposed approach was validated via numerical simulation with a 2-DOF model incorporating an MR damper with the modified hysteretic Dahl model [30] which is a widely used model for hysteretic nonlinearities, and via experimental measurements with a 4-story steel frame building model equipped with two actively-controlled magneto-rheological (MR) dampers, which were employed to simulate nonlinear performance. For comparison, the restoring force of the corresponding linear system was also identified, and then the hysteretic performance of the MR dampers was obtained to validate the accuracy of the identified NRF. The results show that the proposed method is capable of identifying NRF in engineering structures without any assumptions on the structural parameters, and provides a promising approach for damage detection where structural nonlinearity needs to be considered.

2 Formulation and approach

In most of the currently available vibration-based damage detection algorithms, the damage identification is solved as a structural parameters identification and model updating algorithm problem, and the structural damages are evaluated in the form of the variation in structural stiffness. This approach is suitable for linear structures only. Moreover, instead of stiffness, restoring force can describe the linear and nonlinear behavior of the structure or structural members under dynamic loadings directly, and moreover, the hysteresis curve can be employed to evaluate the energy dissipated during vibration and to identify the damage initiation and development quantitatively. Unfortunately, the restoring force of a structure under dynamic loadings cannot be measured directly. Consequently, the efficient and general restoring force identification methodologies using structural dynamic measurements are crucial for damage detection, performance evaluation and remaining service life forecasting of engineering structures.

2.1 Data-based restoring force identification for a nonlinear system under complete excitations

Consider a discrete n-DOF lumped-mass chain-like structural system incorporating nonlinear non-conservative dissipative members and subjected to directly applied forces $F(t)$. The motion of this nonlinear system can be governed by the following equation of motion:

$$M\ddot{x}(t) + R(x, \dot{x}, p) = F(t) \tag{1}$$

where $x(t)$—the displacement vector of order n, M—the constant matrix that characterizes the inertia forces, $R(x, \dot{x}, p)$—the nonlinear non-conservative restoring force vector, p—the vector of system-specific parameters, and $F(t)$—the directly external forces, respectively.

In this study, the NRF of the system is assumed to be expressed in power series polynomial form as shown in the following equation:

$$\begin{aligned} &R_{i,i-1}(x, \dot{x}, p) \\ &\quad \approx R_{i,i-1}(v, s) \\ &\quad \approx \sum_{h=0}^{k} \sum_{j=0}^{q} c^{non}_{i,i-1,h,j} v^{h}_{i,i-1} s^{j}_{i,i-1} \\ &\quad (h \text{ and } j \text{ are not equal to 0 simultaneously}) \end{aligned} \tag{2}$$

where $R_{i,i-1}(x, \dot{x}, p)$ is the NRF between the ith DOF and the $(i-1)$th DOF, $v_{i,i-1}$ and $s_{i,i-1}$ are relative-velocity and relative-displacement vectors (i.e. for a chain-like lumped-mass system, $v_{i,i-1}$ and $s_{i,i-1}$ are the inter-story velocity and inter-story displacement vectors and can be defined as $v_{i,i-1} = \dot{x}_i - \dot{x}_{i-1}, s_{i,i-1} = x_i - x_{i-1}$), $c^{non}_{i,i-1,j,h}$ is the coefficient of the polynomial, and k and q are integers which depend on the nature and extent of the nonlinearity of the system, respectively. Consequently, the equation of motion of the ith DOF can be rearranged as follows:

$$\begin{aligned} &m_i \ddot{x}_i(t) + \sum_{h=0}^{k} \sum_{j=0}^{q} c^{non}_{i,i-1,h,j} v^{h}_{i,i-1} s^{j}_{i,i-1} \\ &\quad + \sum_{h=0}^{k} \sum_{j=0}^{q} c^{non}_{i,i+1,j,h} v^{h}_{i,i+1} s^{j}_{i,i+1} = F_i(t) \end{aligned} \tag{3}$$

Based on the acceleration, relative velocity, relative displacement, and external force time series, the algebraic coefficients used to represent the restoring force,

as well as the mass distribution (m_i), can be identified by means of least-square techniques. Subsequently, the NRF between the ith DOF and the $(i-1)$th DOF can be directly obtained according to (2).

2.2 Data-based restoring force identification for a nonlinear system under incomplete excitations

Since, in practice, it is difficult to excite all of the DOFs of a structure for nonlinearity identification, the above-mentioned methodology should be improved. Consider the nonlinear system mentioned above under arbitrary incomplete excitations, the rank of $F(t)$ defined in (1) will be less than the order of n. Consequently, the unknown coefficients including the mass distribution cannot be uniquely determined by implementing least-square algorithms directly. An updated method which makes use of Newton's third law is thus proposed to handle this situation.

For generality, assume the force is only applied on the ith DOF, and the corresponding coefficients of the ith DOF can be identified from (3). However, the coefficients of the remaining DOFs cannot be uniquely determined due to the right-hand-side (RHS) of the motion equation being zero. According to the relationship between the action force and the reaction force, such an equation exists:

$$\sum_{h=0}^{k}\sum_{j=0}^{q} c_{i,i-1,h,j}^{non} v_{i,i-1}^{h} s_{i,i-1}^{j} = -\sum_{h=0}^{k}\sum_{j=0}^{q} c_{i-1,i,h,j}^{non} v_{i-1,i}^{h} s_{i-1,i}^{j} \tag{4}$$

Hence, the equation of motion of the $(i-1)$th DOF can be rewritten as follows:

$$\begin{aligned} m_{i-1}\ddot{x}_{i-1}(t) + \sum_{h=0}^{k}\sum_{j=0}^{q} c_{i-1,i-2,h,j}^{non} v_{i-1,i-2}^{h} s_{i-1,i-2}^{j} &= -\sum_{h=0}^{k}\sum_{j=0}^{q} c_{i-1,i,j,h}^{non} v_{i-1,i}^{h} s_{i-1,i}^{j} \\ &= \sum_{h=0}^{k}\sum_{j=0}^{q} c_{i,i-1,j,h}^{non} v_{i,i-1}^{h} s_{i,i-1}^{j} \end{aligned} \tag{5}$$

Since the NRF of the ith DOF was previously obtained from (3), the RHS of (5) can be considered as known, and the unknown coefficient of the left-hand side (LHS) can be identified by using least-square techniques. From this point of view, the NRFs of the remaining DOF, on which no external forces are applied, can be identified in sequence.

3 Numerical simulation validation

3.1 2-DOF nonlinear numerical model

To illustrate the accuracy of the method under discussion, a 2-DOF nonlinear lumped-mass structure is considered as an example shown in Fig. 1. Each story of the model is associated with one horizontal DOF. The properties of the structure are $m_i = 10$ kg, $k_i = 1 \times 10^5$ N/m, and $c_i = 100$ N s/m, $(i = 1, 2)$. In order to mimic the nonlinearity, an MR damper, which is widely used as a typical energy dissipation device, is introduced on the 1st floor as shown in Fig. 1.

MR dampers are typical nonlinear members and over the last two decades many numerical models have been proposed to describe their mechanical behavior in parametric or nonparametric forms [1, 4, 18, 19]. In this study a modified Dahl model, which can capture many commonly observed types of hysteretic behavior of MR dampers, is employed [30]. The modified Dahl model is given by the following equations:

$$F_n = K_0 y + C_0 \dot{y} + F_d Z + f_0 \tag{6}$$

$$\dot{Z} = \sigma \dot{y}\left(1 - Z\,\mathrm{sgn}(\dot{y})\right) \tag{7}$$

where K_0—the stiffness coefficient, C_0—the viscous damping coefficient, F_d—the adjustable Coulomb friction, f_0—the initial force, σ—the coefficient used to control the shape of the hysteretic curve, y—the displacement of the damper, and Z—a dimensionless hysteretic parameter which describes the Coulomb

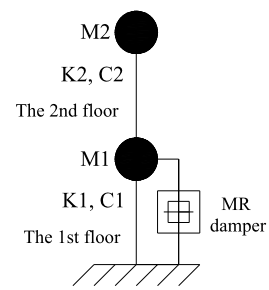

Fig. 1 2-DOF nonlinear numerical model with MR damper

friction. In this example, the following numerical values for the MR damper model are used: $K_0 = 50$ N/m, $C_0 = 399$ N s/m, $F_d = 34.85$ N, $f_0 = 0$ N, and $\sigma = 50{,}000$ s/m.

In order to apply the methodology discussed above, the following basis vectors, which represent the system's acceleration, relative velocity, and relative displacement responses, are selected:

$$\text{Basis} = \{a_1, a_2, v_1, v_2, s_1, s_2\} \tag{8}$$

where a_i—the acceleration of the ith DOF, and $v_i = \dot{x}_i - \dot{x}_{i-1}$ and $s_i = x_i - x_{i-1}$, respectively.

In this study, numerical tests of the frame structure under complete and incomplete random excitations with the considerations of noise-free and 5% noise level in the dynamic response and excitation measurements were carried out. The corresponding responses of the frame structure were obtained by Newmark-β method, and the hysteretic performance of the nonlinear system was identified using the above proposed identification method. The results are discussed in the proceeding sections.

3.2 NRF identification under complete excitations

3.2.1 Case 1: noise-free dynamic responce and exitation measurements

In order to show the effectiveness of the proposed method when all of the DOFs are excited, two random excitations are applied to each floor of the 2-DOF nonlinear model, and the corresponding dynamic responses are determined by numerical integration. In this case, all the responses are assumed to be noise-free. The responses along with their excitations are shown in Fig. 2.

Selecting values for the order $k+q = 3$ of the basis functions in (2) results in the following basis including 9 power series:

$$\text{Basis} = \left\{v, s, v^2, vs, s^2, v^3, v^2 s, vs^2, s^3\right\} \tag{9}$$

According to (3), the applied forces can be fitted as shown in the following equations by using the excitation and response data together with least-squares techniques:

$$\begin{aligned} F_2 = {} & 10.00 \times a_2 + 1.00 \times 10^5 \times s_2 + 100.01 \times v_2 \\ & - 0.05 \times s_2^2 - 6.62 \times 10^{-4} \times s_2 v_2 \\ & - 1.99 \times 10^{-6} \times v_2^2 + 31.03 \times s_2^3 \\ & + 0.08 \times s_2^2 v_2 + 0.01 \times s_2 v_2^2 \\ & - 2.65 \times 10^{-6} \times v_2^3 \end{aligned} \tag{10a}$$

$$\begin{aligned} F_1 = {} & 10.01 \times a_1 - 1.01 \times 10^5 \times s_2 - 96.32 \times v_2 \\ & - 1.15 \times 10^4 \times s_2^2 + 610.32 \times s_2 v_2 \\ & + 5.26 \times v_2^2 - 2.73 \times 10^6 \times s_2^3 \\ & + 1.89 \times 10^3 \times s_2^2 v_2 + 2.26 \times 10^3 \times s_2 v_2^2 \\ & - 6.91 \times v_2^3 + 1.01 \times 10^5 \times s_1 + 666.24 \times v_1 \\ & - 6.77 \times 10^4 \times s_1^2 - 552.97 \times s_1 v_1 \\ & - 7.25 \times v_1^2 + 1.97 \times 10^6 \times s_1^3 \\ & + 5.16 \times 10^5 \times s_1^2 v_1 - 2.83 \times 10^3 \times s_1 v_1^2 \\ & - 332.71 \times v_1^3 \end{aligned} \tag{10b}$$

From the above equations it is worth noting that the identified coefficient of the a_i term stands for the masses of the ith DOF, which are found as $m_2 = 10.00$ and $m_1 = 10.01$, respectively. It is clear that the identified mass distribution is very close to the exact one.

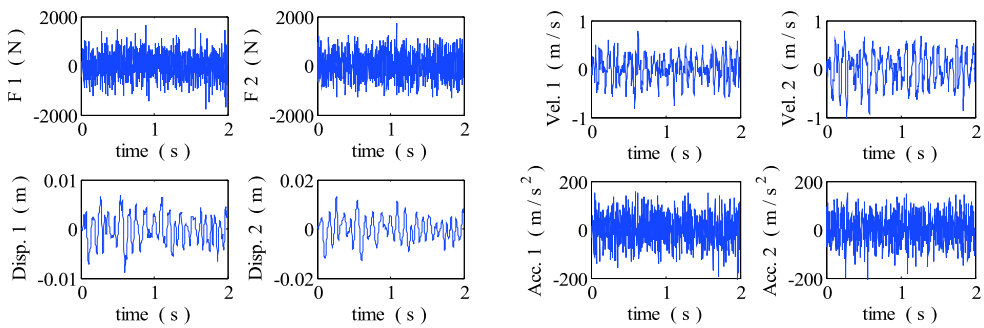

Fig. 2 The random excitations applied to each floor of the system and the corresponding responses

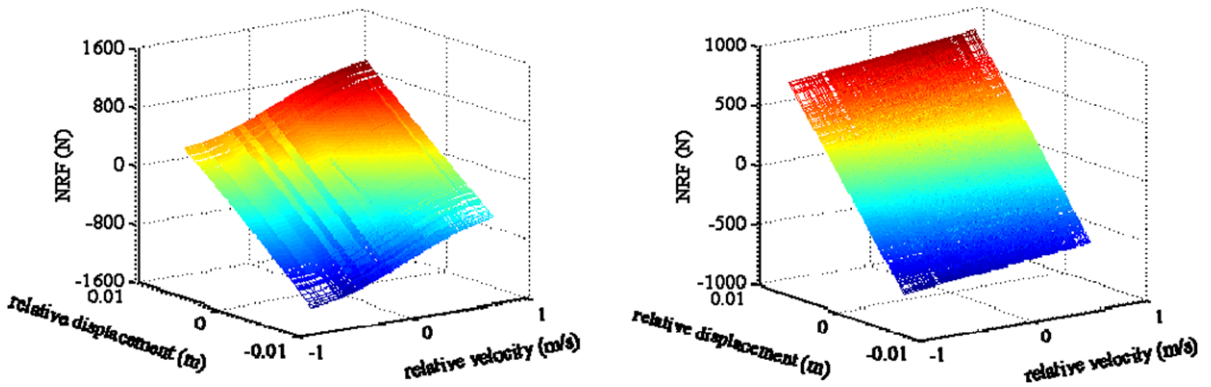

Fig. 3 The identified NRF under complete exitations (noise-free): (**a**) on the 1st floor, (**b**) on the 2nd floor

Moreover, the NRFs can be easily obtained according to (2)–(3) and can be shown in the following equations:

$$\begin{aligned} &R_{2,1}^{non}(s_2, v_2) \\ &\quad = 1.00 \times 10^5 \times s_2 + 100.01 \times v_2 - 0.05 \times s_2^2 \\ &\qquad - 6.62 \times 10^{-4} \times s_2 v_2 - 1.99 \times 10^{-6} \times v_2^2 \\ &\qquad + 31.03 \times s_2^3 + 0.08 \times s_2^2 v_2 \\ &\qquad + 0.01 \times s_2 v_2^2 - 2.65 \times 10^{-6} \times v_2^3 \end{aligned} \tag{11a}$$

$$\begin{aligned} &R_{1,0}^{non}(s_1, v_1) \\ &\quad = 1.01 \times 10^5 \times s_1 + 666.24 \times v_1 \\ &\qquad - 6.77 \times 10^4 \times s_1^2 - 552.97 \times s_1 v_1 \\ &\qquad - 7.25 \times v_1^2 + 1.97 \times 10^6 \times s_1^3 \\ &\qquad + 5.16 \times 10^5 \times s_1^2 v_1 - 2.83 \times 10^3 \times s_1 v_1^2 \\ &\qquad - 332.71 \times v_1^3 \end{aligned} \tag{11b}$$

Based on the above established power series polynomial models of NRF, the extent and characteristics of the nonlinearity can be represented more clearly in three-dimensional graphs that illustrate the relation between the restoring force and relative displacement and velocity as shown in Fig. 3. From these graphs it is obvious that the restoring force surface is non-planar on the 1st floor and planar on the 2nd floor. This means that the MR damper is influencing the response of the 1st floor but not influencing the response of the 2nd floor. Also, together with time matching techniques, these polynomial models can be used to track the nonlinear performance of the structure in the time domain.

Since the identified NRF is equal to the summation of the elastic restoring force, the damping effects of the structure, and the nonlinear member force, the MR damper force can be determined by subtracting the linear elastic restoring force and damping force of the structure alone from the identified total restoring force. The result can then be used to validate the accuracy of the identified NRF. The MR damper force is shown in Fig. 4. Note that identical amplitude scales are applied to all the plots.

From Fig. 4 it is easily seen that the MR damper is located on the 1st floor as the identified MR damper forces on the 2nd floor are close to zero. Next, in order to evaluate the accuracy of the proposed method for the MR force identification, the MR damper force determined by the proposed method is compared with that determined by its numerical model given by (6)–(7). It is obvious that the identified MR damper force is close to the simulated one from Fig. 4(a). It means that the identified power series polynomial model can be used to represent the NRFs effectively and that the proposed method provides a suitable way to identify the NRF of the system.

3.2.2 Additional case: 5% noise level in dynamic response and excitation measurements

Another set of unrelated random excitations is applied to the nonlinear numerical model and the corresponding responses are obtained. As a practical consideration, noise is expected in the output and input measurements. Without loss of generality, in this additional case the noise level is set to be 5%, which means the

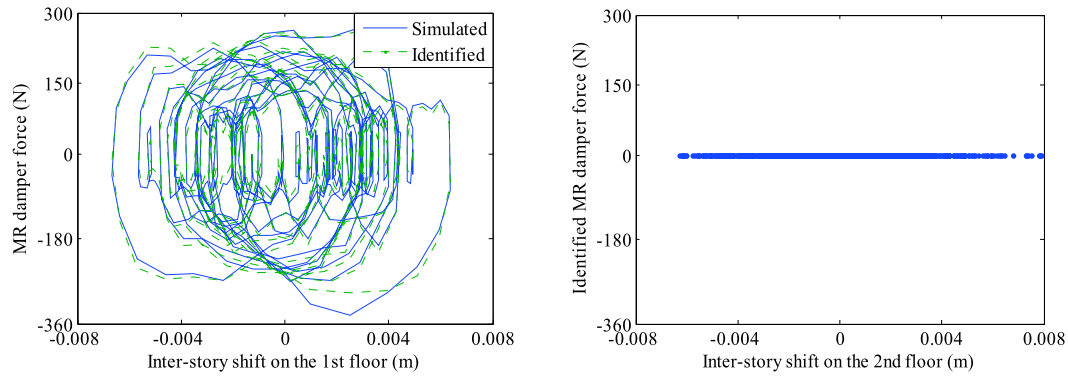

Fig. 4 The MR damper force under complete excitations (noise-free): (**a**) on the 1st floor; (**b**) on the 2nd floor

standard deviation of the random noise is equal to 5% of the corresponding mean value. Similar procedures shown in the previous section are implemented to identify the NRF of the system and MR damper force. The identified NRFs are given in (12a)–(12b) and the MR damper forces in this case are plotted in Fig. 5. It is obvious from Fig. 5 that the MR damper is fixed on the 1st floor and the identified MR force has good agreement with the simulated one even when the response measurements are contaminated by 5% noise.

$$
\begin{aligned}
&R_{2,1}^{non}(s_2, v_2)\\
&\quad = 9.96 \times 10^4 \times s_2 + 95.24 \times v_2 - 6.23 \times 10^4 \times s_2^2\\
&\qquad + 276.54 \times s_2 v_2 - 2.90 \times v_2^2 - 2.75 \times 10^6 \times s_2^3\\
&\qquad - 1.45 \times 10^4 \times s_2^2 v_2 + 140.75 \times s_2 v_2^2\\
&\qquad + 7.89 \times v_2^3 \qquad (12a)
\end{aligned}
$$

$$
\begin{aligned}
&R_{1,0}^{non}(s_1, v_1)\\
&\quad = 9.87 \times 10^4 \times s_1 + 564.95 \times v_1\\
&\qquad - 2.12 \times 10^4 \times s_1^2 - 1.15 \times 10^3 \times s_1 v_1\\
&\qquad - 1.63 \times v_1^2 - 1.08 \times 10^6 \times s_1^3\\
&\qquad - 1.89 \times 10^5 \times s_1^2 v_1 + 423.82 \times s_1 v_1^2\\
&\qquad - 35.75 \times v_1^3 \qquad (12b)
\end{aligned}
$$

3.3 NRF identification under incomplete excitations

3.3.1 Case 1: noise-free dynamic response and excitation measurements

In order to verify the performance of the proposed approach for nonlinearity identification when only part of the DOFs of the object structure are excited, the 2nd floor of the nonlinear numerical model shown in Fig. 1 is assumed to be excited by a set of random excitations. The corresponding responses of the system are also determined by the Newmark-β method and considered to be noise-free in this case. Based on the time-domain measurements of the excitation and the response, the expression of the force applied on the 2nd floor can be determined according to (3) as:

$$
\begin{aligned}
F_2 &= 10.00 \times a_2 + 1.00 \times 10^5 \times s_2 + 100.01 \times v_2\\
&\quad - 0.07 \times s_2^2 + 0.01 \times s_2 v_2 - 7.86 \times 10^{-6} \times v_2^2\\
&\quad + 56.68 \times s_2^3 + 0.42 \times s_2^2 v_2 - 0.01 \times s_2 v_2^2\\
&\quad - 2.34 \times 10^{-5} \times v_2^3 \qquad (13)
\end{aligned}
$$

It is then easy to obtain $m_2 = 10.00$, and the NRF on the 2nd floor is

$$
\begin{aligned}
&R_{2,1}^{non}(s_2, v_2)\\
&\quad = 1.00 \times 10^5 \times s_2 + 100.01 \times v_2 - 0.07 \times s_2^2\\
&\qquad + 0.01 \times s_2 v_2 - 7.86 \times 10^{-6} \times v_2^2\\
&\qquad + 56.68 \times s_2^3 + 0.42 \times s_2^2 v_2 - 0.01 \times s_2 v_2^2\\
&\qquad - 2.34 \times 10^{-5} \times v_2^3 \qquad (14)
\end{aligned}
$$

Since $R_{2,1}^{non}(s_2, v_2)$ is determined, the motion of equation of the 1st DOF can be rearranged according to (4)–(5):

$$
\begin{aligned}
&m_1 a_1 + \sum_{h=0}^{k} \sum_{j=0}^{q} c_{1,0,h,j}^{non} v_1^h s_1^j = R_{2,1}^{non}(s_2, v_2),\\
&(k + q = 3) \qquad (15)
\end{aligned}
$$

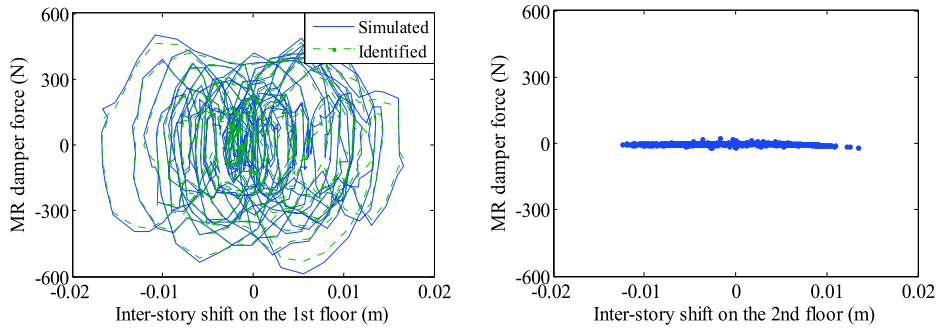

Fig. 5 The MR damper force under complete excitations (5% noise): (**a**) on the 1st floor, (**b**) on the 2nd floor

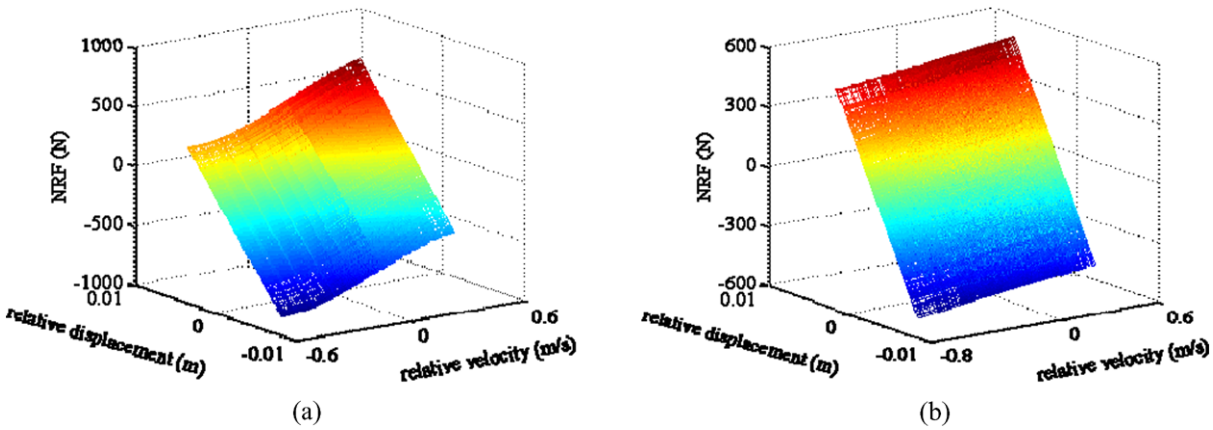

Fig. 6 The identified NRFs under incomplete excitations (noise-free): (**a**) on the 1st floor, (**b**) on the 2nd floor

Based on the responses of the system and the identified $R_{2,1}^{non}(s_2, v_2)$, the unknown coefficients in the LHS of (15) can be identified. Consequently, the lumped mass can be found as $m_1 = 9.85$. Also, the NRF on the 1st floor is given by

$$\begin{aligned} &R_{1,0}^{non}(s_1, v_1) \\ &= 0.98 \times 10^5 \times s_1 + 749.74 \times v_1 \\ &\quad + 1.60 \times 10^5 \times s_1^2 + 5.02 \times 10^3 \times s_1 v_1 \\ &\quad - 68.26 \times v_1^2 + 1.71 \times 10^7 \times s_1^3 \\ &\quad + 1.27 \times 10^5 \times s_1^2 v_1 + 9.52 \times 10^3 \times s_1 v_1^2 \\ &\quad - 1.04 \times 10^3 \times v_1^3 \end{aligned} \tag{16}$$

The three-dimensional graph in the form of the identified NRF plotted against the relative displacement and relative velocity is shown in Fig. 6, and clearly represents the nonlinearity of the system in this case. The similar conclusion that the MR damper is located on the 1st floor can be obtained by comparing these NRF surfaces.

Since the NRF is determined, the MR damper force can be obtained accordingly. The identified MR forces as well as the simulated forces are displayed in Fig. 7. From this figure it can again be concluded that the MR damper is located on the 1st floor. Moreover, it is clear from the results displayed in Fig. 7(a) that the modeling approach under discussion yields reasonably accurate fidelity in the identification of the NRF even under incomplete excitations.

3.3.2 *Additional case: 5% noise level in dynamic response and excitation measurements*

To investigate the effect of the noise on the identification of NRFs while the system is partially excited,

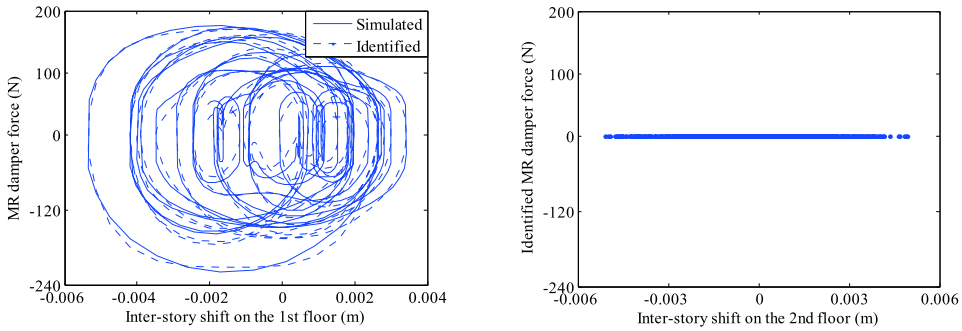

Fig. 7 The MR damper force under incomplete excitations (noise-free): (**a**) on the 1st floor; (**b**) on the 2nd floor

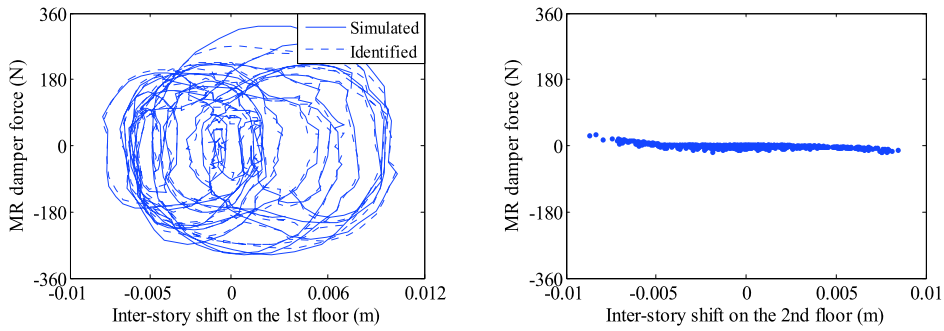

Fig. 8 The MR damper force under incomplete excitations (5% noise): (**a**) on the 1st floor; (**b**) on the 2nd floor

an additional case in which the excitations and the corresponding responses are polluted by 5% noise is discussed. The numerical model shown in Fig. 1 is excited on the 2nd floor by another set of random forces. Based on the external excitation and the contaminated responses, the similar procedures carried out in Sect. 3.3.1 are implemented and the NRFs of the structure are identified as shown in (17a)–(17b).

$$
\begin{aligned}
&R_{2,1}^{non}(s_2, v_2)\\
&\quad = 1.02 \times 10^5 \times s_2 + 97.73 \times v_2\\
&\qquad + 1.79 \times 10^5 \times s_2^2\\
&\qquad + 103.36 \times s_2 v_2 - 27.49 \times v_2^2\\
&\qquad - 7.38 \times 10^7 \times s_2^3 + 9.12 \times 10^5 \times s_2^2 v_2\\
&\qquad + 2.74 \times 10^3 \times s_2 v_2^2 + 11.47 \times v_2^3 \qquad (17a)
\end{aligned}
$$

$$
\begin{aligned}
&R_{1,0}^{non}(s_1, v_1)\\
&\quad = 9.92 \times 10^4 \times s_1 + 652.72 \times v_1\\
&\qquad + 2.46 \times 10^4 \times s_1^2 + 1.71 \times 10^3 \times s_1 v_1\\
&\qquad + 3.70 \times v_1^2 - 1.13 \times 10^7 \times s_1^3\\
&\qquad - 3.91 \times 10^5 \times s_1^2 v_1 - 8.43 \times 10^3 \times s_1 v_1^2\\
&\qquad - 340.31 \times v_1^3 \qquad (17b)
\end{aligned}
$$

Since the NRFs are determined, the hysteretic performance of the MR damper can be obtained and used to validate the accuracy of the identified NRFs. The identified MR force is plotted in Fig. 8 and the simulated MR force is also shown in Fig. 8 for comparison. It can be observed that though the excitations and responses are contaminated by 5% noise, the proposed approach is still capable of identifying the nonlinear performance of the system with acceptable accuracy under incomplete excitations.

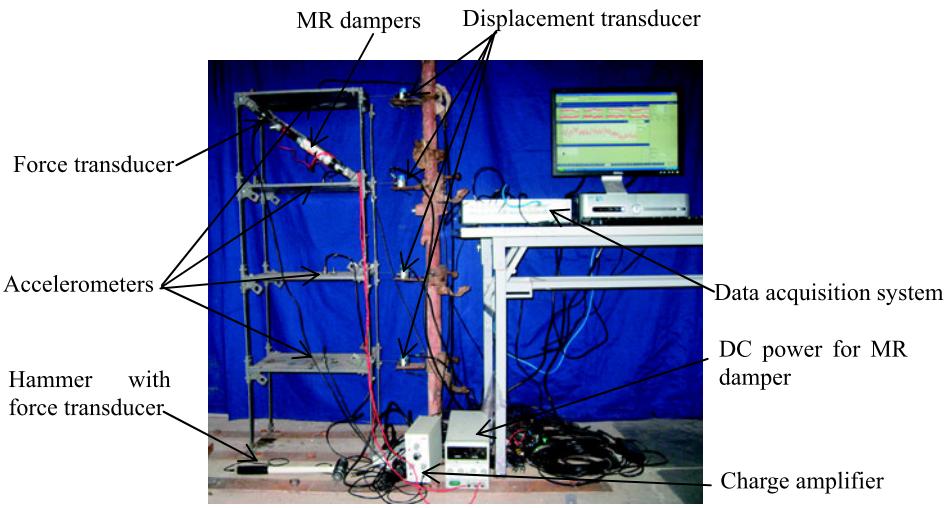

Fig. 9 Nonlinear multi-story structure with MR dampers and vibration test setup

4 Test validation

4.1 Model structure and forced vibration test

To illustrate the application of the proposed method in conjunction with a real structure, a four-story steel frame building model with two MR dampers was constructed in the lab and used to conduct forced vibration tests. The structure is 0.3 m × 0.4 m in plane, 1.2 m in height, distributed evenly among the four floors, and has a total mass of 51.41 kg. The cross section of the columns is 30 mm × 5 mm, and the thickness of the floor plates is 10 mm. All the joints are connected using bolts.

Two MR dampers with an input current of 0.1 A were installed on the 4th floor to induce a nonlinear hysteretic restoring force. An impact hammer was employed to excite the structure and the excitation force was measured directly by a piezoelectric force gauge in the hammer. The corresponding acceleration and displacement responses of the four stories were measured directly by four accelerometers and four displacement transducers, respectively. The excitations and the acceleration and displacement responses were recorded simultaneously with a sampling frequency of 1024 Hz. The velocity response of the structure was obtained by numerical integration of the measured accelerations. To eliminate the influence of measurement noise, a high-pass filter with a pass frequency of 1 Hz was employed to process the acceleration measurements. For comparison, the damping force of the MR damper was measured by a piezoelectric force gauge.

4.2 Nonlinear restoring force identification under complete excitations in the lab

4.2.1 Nonlinear restoring force identification of the structure with MR dampers

In this case, the four floors of the model structure were excited by the hammer in a horizontal direction. The impact forces and the corresponding responses are all plotted in Fig. 10.

Let the sum of the integers k and q of the power series polynomial given in (2) be equal to 3. Based on the time-domain information of the system's excitations and responses, the expressions of external excitations can be fitted using least-square techniques. The same procedures shown in the preceding numerical example were implemented to obtain the inter-story NRF as well as the mass distribution of the structure. The identified results of the mass are $m_1 = 12.53$ kg, $m_2 = 12.41$ kg, $m_3 = 12.47$ kg and $m_4 = 12.16$ kg, respectively. Also, the polynomial models of the inter-story NRF are determined and shown by

$$\begin{aligned} R_{4,3}^{non}(s_4, v_4) &= 1.49 \times 10^5 \times s_4 + 354.75 \times v_4 \\ &\quad - 6.88 \times 10^5 \times s_4^2 + 2.18 \times 10^4 \times s_4 v_4 \\ &\quad - 72.42 \times v_4^2 + 4.11 \times 10^9 \times s_4^3 \end{aligned}$$

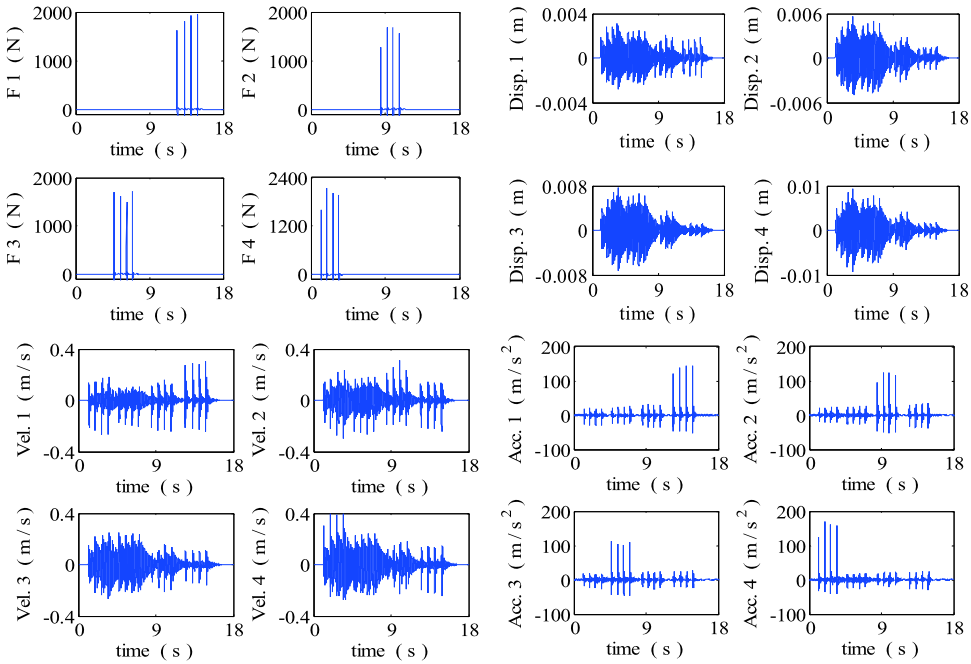

Fig. 10 Impact forces applied to each floor of the nonlinear system and the corresponding responses

$$
\begin{aligned}
&- 3.89 \times 10^7 \times s_4^2 v_4 + 1.13 \times 10^5 \times s_4 v_4^2 \\
&- 2.65 \times 10^3 \times v_4^3 \qquad (18a)
\end{aligned}
$$

$$
\begin{aligned}
&R_{3,2}^{non}(s_3, v_3) \\
&= 1.34 \times 10^5 \times s_3 + 22.02 \times v_3 - 1.25 \times 10^6 \times s_3^2 \\
&+ 4.64 \times 10^4 \times s_3 v_3 - 187.77 \times v_3^2 \\
&+ 2.69 \times 10^9 \times s_3^3 - 2.45 \times 10^6 \times s_3^2 v_3 \\
&+ 2.09 \times 10^5 \times s_3 v_3^2 - 132.48 \times v_3^3 \qquad (18b)
\end{aligned}
$$

$$
\begin{aligned}
&R_{2,1}^{non}(s_2, v_2) \\
&= 1.39 \times 10^5 \times s_2 + 16.11 \times v_2 - 4.12 \times 10^5 \times s_2^2 \\
&- 2.20 \times 10^4 \times s_2 v_2 - 50.73 \times v_2^2 \\
&- 4.96 \times 10^8 \times s_2^3 + 2.70 \times 10^6 \times s_2^2 v_2 \\
&+ 1.06 \times 10^5 \times s_2 v_2^2 + 193.31 \times v_2^3 \qquad (18c)
\end{aligned}
$$

$$
\begin{aligned}
&R_{1,0}^{non}(s_1, v_1) \\
&= 1.35 \times 10^5 \times s_1 + 30.35 \times v_1 + 5.47 \times 10^5 \times s_1^2 \\
&- 6.55 \times 10^4 \times s_1 v_1 - 101.36 \times v_1^2 \\
&- 4.17 \times 10^8 \times s_1^3 + 1.73 \times 10^6 \times s_1^2 v_1 \\
&- 3.84 \times 10^5 \times s_1 v_1^2 + 1.05 \times 10^5 \times v_1^3 \qquad (18d)
\end{aligned}
$$

Figure 11 shows the relationship between the identified total restoring force and the inter-story displacement and inter-story velocity of the nonlinear model structure. From Fig. 11 it is clear that typical nonlinear characteristics exist on the 4th floor and the NRF surfaces of the remaining floors are close to planar, thus implying that they behave linearly. In some cases, such as post-event damage detection, the identified NRF of the object structure may be the end result that is required, and no further identification tasks need be implemented. Through the analysis of the identified inter-story NRF together with time matching techniques, the extent of the nonlinearity, the time of the damage initiation and development, and the energy dissipation during vibration can be identified.

As mentioned before, the total inter-story NRF identified above consists of the elastic restoring force, viscous damping force, and the MR damper force, therefore it usually cannot be measured directly. In this study, the performance of the proposed approach was verified by comparing the identified MR damper force with the test measurements. In order to identify the MR damper force, the elastic restoring force and the viscous damping force provided by the structure itself should be subtracted from the total identified NRFs. Consequently, the above proposed methodology was

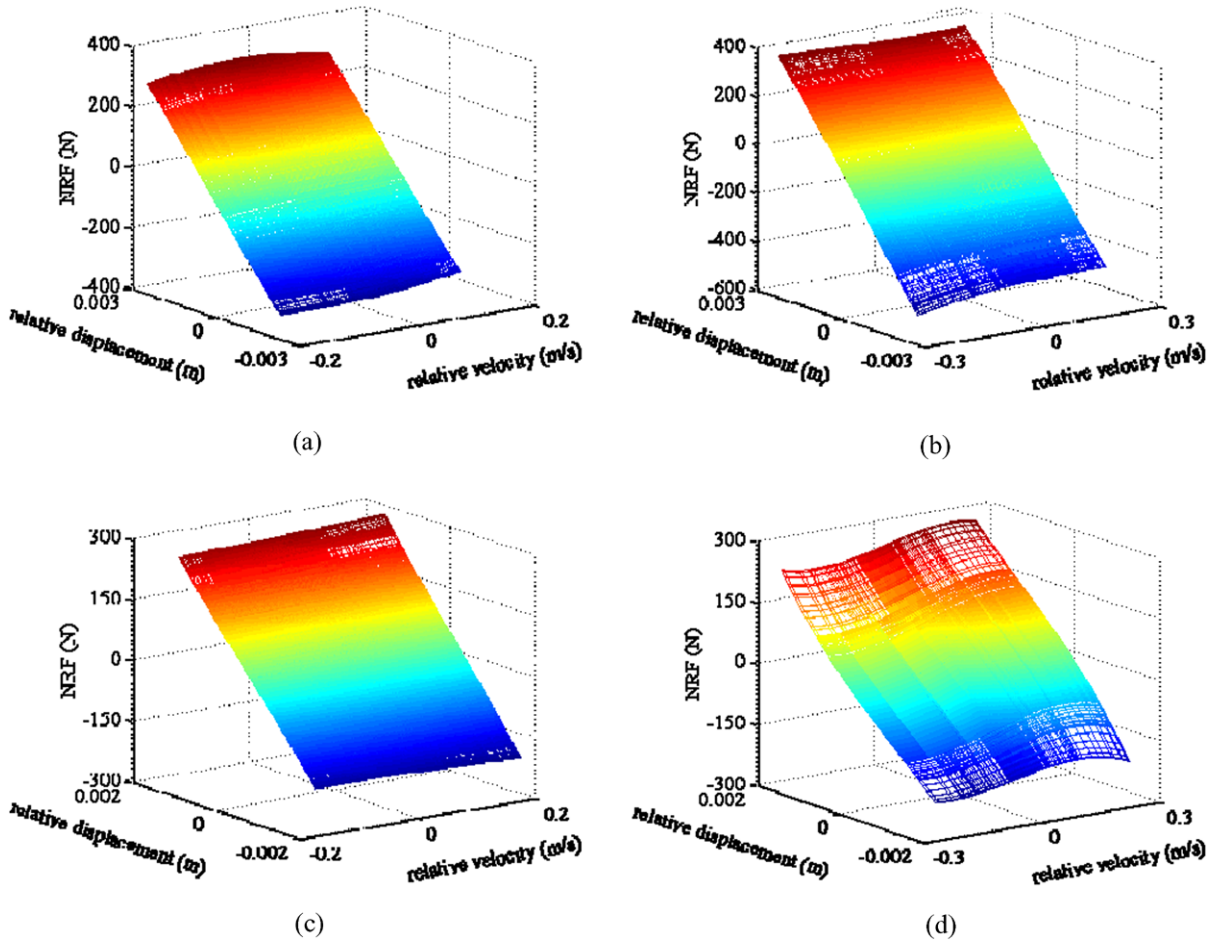

Fig. 11 The identified NRFs: (**a**) on the 1st floor, (**b**) on the 2nd floor, (**c**) on the 3rd floor, (**d**) on the 4th floor

employed to identify the parameters of the linear structure without the MR dampers.

4.2.2 *Identification for linear structure*

In order to identify the elastic stiffness and damping coefficients of the structure, the two MR dampers were removed from the model structure and similar forced vibration tests were carried out. The external force applied to the corresponding linear system is $P(t)$. The method described in (2) is employed to identify the linear system without the MR dampers. Let $k+q=1$ in (2), (3) can be rewritten as follows:

$$m_i\ddot{x}_i(t)+\sum_{h=0}^{k'}\sum_{j=0}^{q'}c^{lin}_{i,i-1,h,j}v^h_{i,i-1}s^j_{i,i-1}+\sum_{h=0}^{k'}\sum_{j=0}^{q'}c^{lin}_{i,i+1,j,h}v^h_{i,i+1}s^j_{i,i+1}=P_i(t)$$
$$(k'+q'=1) \tag{19}$$

Similarly, based on the time-domain vectors, each coefficient of the linear system ($c^{lin}_{i,i-1,j,h}$ and $c^{lin}_{i,i+1,j,h}$) can be identified by using least-square estimation methods. The identified restoring force of the linear model can be expressed as follows:

$$R^{lin}_{4,3}(s_4,v_4)=1.37\times10^5\times s_4+19.25\times v_4 \tag{20a}$$
$$R^{lin}_{3,2}(s_3,v_3)=1.45\times10^5\times s_3+26.63\times v_3 \tag{20b}$$
$$R^{lin}_{2,1}(s_2,v_2)=1.48\times10^5\times s_2+14.77\times v_2 \tag{20c}$$
$$R^{lin}_{1,0}(s_1,v_1)=1.31\times10^5\times s_1+24.09\times v_1 \tag{20d}$$

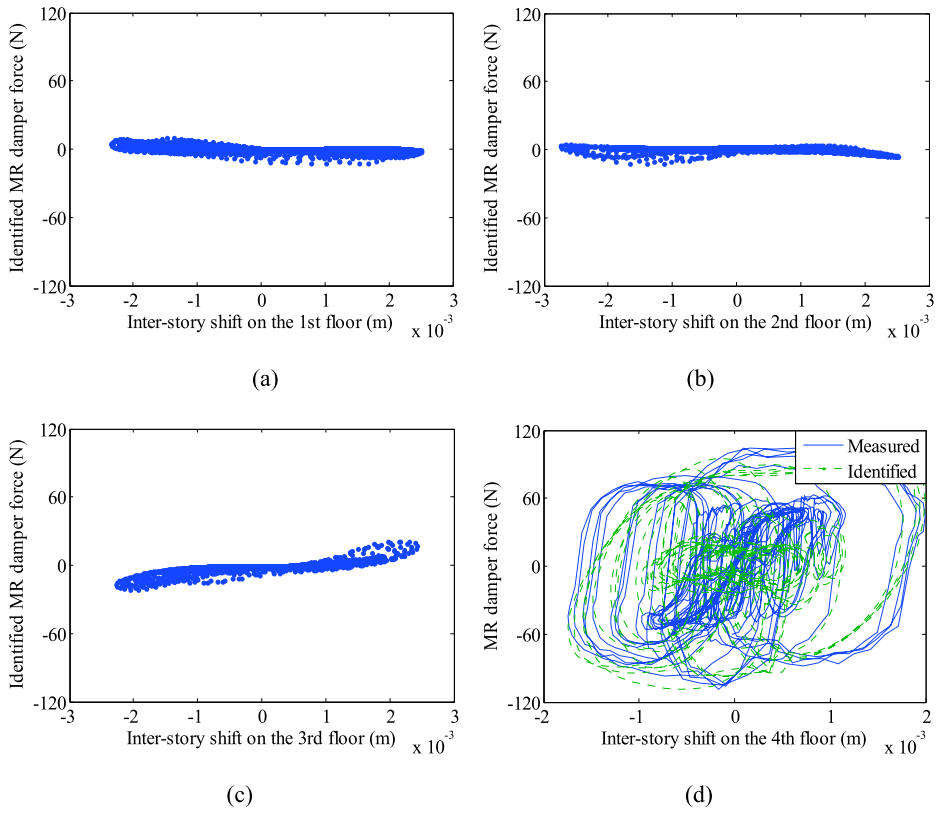

Fig. 12 The MR damper force: (**a**) on the 1st floor; (**b**) on the 2nd floor; (**c**) on the 3rd floor; (**d**) on the 4th floor

Moreover, according to (19), the mass distribution of the linear structure can be identified as $m_1 = 12.33$ kg, $m_2 = 12.28$ kg, $m_3 = 12.24$ kg, and $m_4 = 12.09$ kg. It is obvious that the identified masses of the linear structure are close to the nonlinear structure, because the mass of the employed MR dampers in this model structure is only 0.4 kg, which is much smaller than the mass of the frame structure, and therefore has little influence on the structural mass distribution.

4.2.3 MR damper force identification and comparison

Next, the nonlinear force (i.e. MR damper force in this study) between the ith DOF and the $(i-1)$ th DOF can be extracted from the total NRFs through the following equation:

$$F_{non} = \sum_{h=0}^{k}\sum_{j=0}^{q} c^{non}_{i,i-1,h,j} v^{h}_{i,i-1} s^{j}_{i,i-1} - \sum_{h=0}^{k'}\sum_{j=0}^{q'} c^{lin}_{i,i-1,h,j} v^{h}_{i,i-1} s^{j}_{i,i-1}, \quad (k'+q'=1) \tag{21}$$

Since the NRFs and linear restoring forces (LRFs) are determined in (18a)–(18d) and (20a)–(20d), the MR damper force can be identified and is displayed in Fig. 12. For comparison, the measured MR damper force is also shown in Fig. 12. It should be noted that the force gauge as shown in Fig. 9 is diagonal, but the identified MR forces obtained from (21) are in the horizontal direction, so the component in the horizontal direction of the measured MR force is the value to be compared with the identified results. It is obvious that the MR dampers are not placed on the 1st, 2nd and 3rd floors because the identified MR forces on these floors are very small. By comparing the identified MR damping force with the measured damping force as shown in Fig. 12(d), it can be concluded that the proposed method provides a reasonably accurate identification

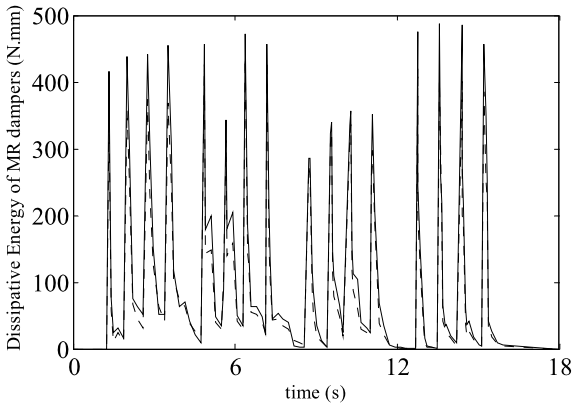

Fig. 13 The comparison of dissipative energy: *solid line* corresponds to the measured MR force; *dashed line*, to the identified one

of the NRF, both qualitatively and quantitatively, even when no information about the system's topology, or about the nature of element forces, is utilized.

In practice, the energy of the structural member absorbed, which depends on the area of the hysteretic loops during the dynamic excitation, is a direct index for damage detection. In this study, the accuracy of the identified non-conservative restoring force was also evaluated in the form of energy dissipation during the vibration test. The comparison of the dissipated energy of the MR dampers determined by the identified damper forces with that determined by the force measurements is shown in Fig. 13. It is clear that the identified energy dissipation is very close to that obtained from the measurements. This finding means that the proposed approach has potential to be applied in practice to evaluate the structural post-event damage which is related to the energy dissipation during dynamic excitation such as earthquakes.

4.3 NRF identification under incomplete excitations

4.3.1 Nonlinear restoring force identification of the structure with MR dampers

Here, the validity of the improved approach for the identification of NRF while the structure is under incomplete excitations, with only the 3rd floor of the structure being excited, is studied. Based on the impact force, measured acceleration, integrated velocity, and measured displacement, the expression of the force applied on the 3rd floor can be obtained by least-square techniques. Subsequently, according to (4)–(5), the mass is known as $m_3 = 12.41$ kg and the NRFs are given by

$$\begin{aligned} &R_{4,3}^{non}(s_4, v_4) \\ &\quad = 1.37 \times 10^5 \times s_4 + 320.16 \times v_4 \\ &\qquad - 9.68 \times 10^5 \times s_4^2 + 9.03 \times 10^4 \times s_4 v_4 \\ &\qquad + 248.69 \times v_4^2 + 3.27 \times 10^9 \times s_4^3 \\ &\qquad - 2.61 \times 10^7 \times s_4^2 v_4 - 4.43 \times 10^5 \times s_4 v_4^2 \\ &\qquad + 1.56 \times 10^3 \times v_4^3 \end{aligned} \tag{22a}$$

$$\begin{aligned} &R_{3,2}^{non}(s_3, v_3) \\ &\quad = 1.41 \times 10^5 \times s_3 + 20.58 \times v_3 - 9.11 \times 10^5 \times s_3^2 \\ &\qquad + 1.93 \times 10^4 \times s_3 v_3 + 480.82 \times v_3^2 \\ &\qquad + 5.17 \times 10^9 \times s_3^3 + 2.68 \times 10^6 \times s_3^2 v_3 \\ &\qquad - 4.82 \times 10^5 \times s_3 v_3^2 - 515.44 \times v_3^3 \end{aligned} \tag{22b}$$

Similarly to the numerical example discussed above, the NRFs of the remaining floors as well as the masses are determined in sequence. The identified masses are $m_4 = 12.84$ kg, $m_2 = 13.00$ kg and $m_1 = 12.97$ kg, respectively. The identified NRFs are shown as follows:

$$\begin{aligned} &R_{2,1}^{non}(s_2, v_2) \\ &\quad = 1.31 \times 10^5 \times s_2 + 16.29 \times v_2 + 1.96 \times 10^6 \times s_2^2 \\ &\qquad - 1.52 \times 10^4 \times s_2 v_2 + 124.84 \times v_2^2 \\ &\qquad - 2.38 \times 10^9 \times s_2^3 + 2.31 \times 10^7 \times s_2^2 v_2 \\ &\qquad - 9.76 \times 10^4 \times s_2 v_2^2 + 266.51 \times v_2^3 \end{aligned} \tag{22c}$$

$$\begin{aligned} &R_{1,0}^{non}(s_1, v_1) \\ &\quad = 1.32 \times 10^5 \times s_1 + 52.50 \times v_1 + 1.78 \times 10^6 \times s_1^2 \\ &\qquad - 8.47 \times 10^4 \times s_1 v_1 - 128.72 \times v_1^2 \\ &\qquad - 2.19 \times 10^8 \times s_1^3 + 2.19 \times 10^7 \times s_1^2 v_1 \\ &\qquad - 4.28 \times 10^5 \times s_1 v_1^2 + 210.84 \times v_1^3 \end{aligned} \tag{22d}$$

The identified NRFs shown in (22a)–(22d) are plotted against the relative displacement and relative velocity and are displayed in Fig. 14. It is obvious that the NRF surfaces are approximately planar except for the surface associated with the 4th floor, indicating that the MR dampers are placed on the 4th floor.

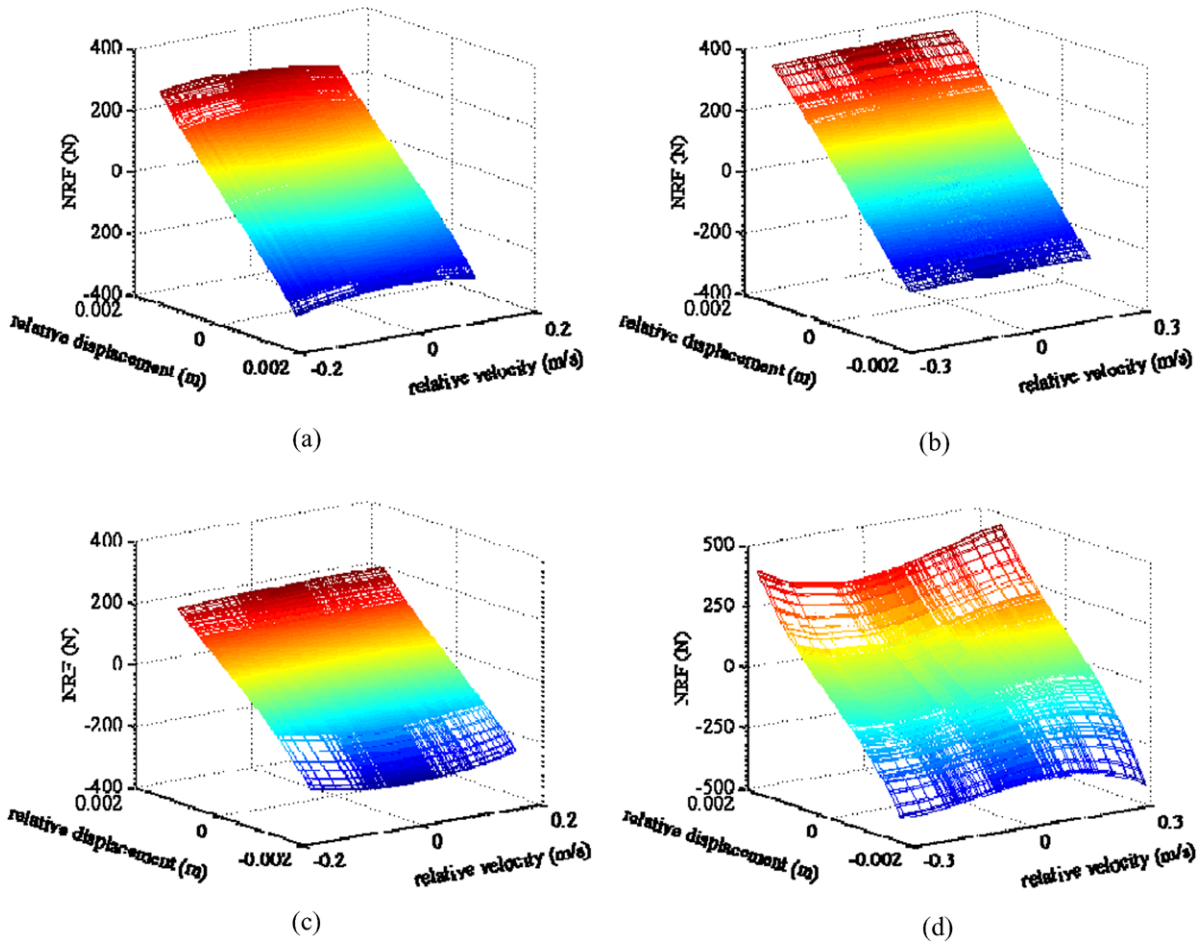

Fig. 14 The identified NRFs: (**a**) on the 1st floor, (**b**) on the 2nd floor, (**c**) on the 3rd floor, (**d**) on the 4th floor

4.3.2 Identification for linear structure

In this case, without loss of generality, only the second floor of the corresponding linear model structure is excited, and the corresponding acceleration, displacement measurements, and excitation force are recorded. Let $k + q = 1$ and the corresponding linear coefficients of the ith DOF can be identified from (3)–(5). The mass distribution of the linear structure is found as $m_1 = 12.35$ kg, $m_2 = 12.11$ kg, $m_3 = 12.56$ kg and $m_4 = 12.66$ kg, respectively. The restoring forces of the linear structure are identified as

$$R^{lin}_{4,3}(s_4, v_4) = 1.37 \times 10^5 \times s_4 + 23.36 \times v_4 \quad (23a)$$

$$R^{lin}_{3,2}(s_3, v_3) = 1.46 \times 10^5 \times s_3 + 27.32 \times v_3 \quad (23b)$$

$$R^{lin}_{2,1}(s_2, v_2) = 1.49 \times 10^5 \times s_2 + 13.06 \times v_2 \quad (23c)$$

$$R^{lin}_{1,0}(s_1, v_1) = 1.26 \times 10^5 \times s_1 + 12.25 \times v_1 \quad (23d)$$

It can be easily found that the coefficients shown in (23a)–(23d) are close to those shown in (20a)–(20d), indicating that the proposed polynomial model can be used to represent the restoring force of the linear system $k + q = 1$ under both complete and incomplete excitations.

4.3.3 MR damper force identification and comparison

Similarly to the case of complete excitations, the MR damper force was measured and compared with the identified force in order to validate the accuracy of proposed method. According to (21), the MR damper

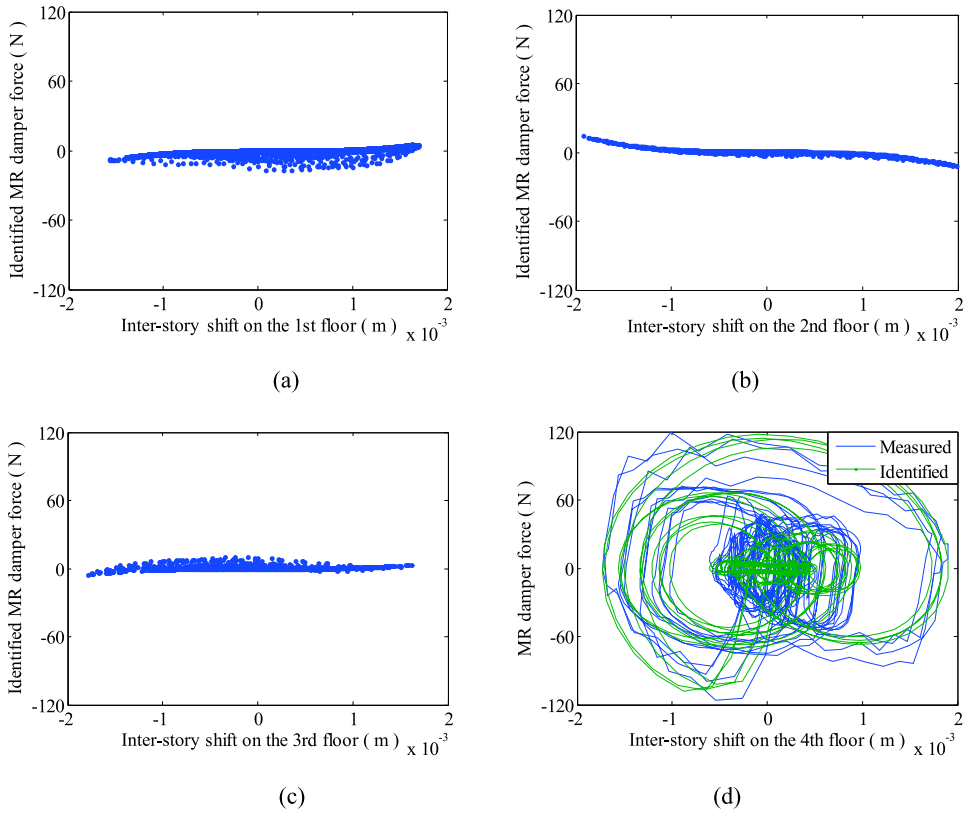

Fig. 15 The MR damper force: (**a**) on the 1st floor; (**b**) on the 2nd floor; (**c**) on the 3rd floor; (**d**) on the 4th floor

forces can be determined and plotted in Fig. 15. Since the MR damper force on the 1st, 2nd, and 3rd floors are very small, it can easily be concluded that there are no dampers located there. For comparison, the horizontal component of the measured MR force on the 4th floor is also shown in Fig. 15. It is clear that the identified MR damper force has good agreement with the measured one, even though there are differences between their shapes.

Also, the comparison of the dissipative energy determined by the identified damper force and the measurements is presented in Fig. 16. Even though a little difference exists between the shapes of the two curves shown in Fig. 15(d), the identified energy dissipation of the dampers during vibration is very close to that determined by measurements. This means that though the excitations are incomplete, the proposed updated method is still capable of identifying the NRF, locating damages, and even assessing the extent of the damage.

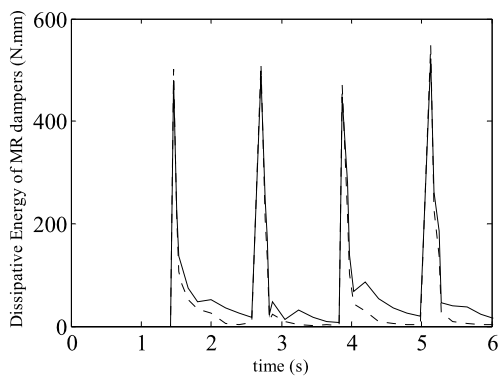

Fig. 16 The comparison of dissipative energy: *solid line* corresponds to the measured MR force; *dashed line*, to the identified force

5 Concluding remarks

A power series polynomial modeling technique is presented for the identification of NRF of chain-like multi-degree-of-freedom system while the nonlinear

dynamic system is under complete or incomplete excitations. The feasibility and robustness of the proposed method is validated via numerical simulation with a 2-DOF system incorporating a parametric MR model, and via an experiment with a 4-story steel frame structure equipped with two actively-controlled MR dampers. Results show that the identified polynomial models can capture the dominant features of the exact nonlinear system and the proposed methodology can be suitable for linear and nonlinear dynamic systems.

A distinguishing feature of the proposed modeling approach is that, other than the assumption of chain-like topology, it does not need information about the structure (such as structural characteristics or model-class) and only the applied excitations and corresponding responses are required. It provides a general methodology for the identification of NRFs of engineering structures, which can be used for monitoring of damage initiation and development and evaluation of damage severity of engineering structures under dynamic loadings, where significant nonlinearities may be induced. Further study on the performance of the proposed approach for dynamic system with parameters varying with time during the shaking event should be carried out in the future.

Acknowledgements The authors gratefully acknowledge the support provided through the National Natural Science Foundation of China (NSFC) under Grants Nos. 50608031 and 50978092 and the Hunan Provincial Natural Science Foundation of China under Grant No. 08JJ1009. Partial support by Program for New Century Excellent Talents in University (NCET-08-0178) is also greatly appreciated.

References

1. Dahl, P.R.: Solid friction damping of mechanical vibrations. AIAA J. **14**(12), 1675–1682 (1976)
2. Doebling, S.W., Farrar, C.R., Prime, M.B., Shevitz, D.W.: A review of damage identification methods that examine changes in dynamic properties. Shock Vib. Dig. **30**(2), 91–105 (1998)
3. Ghanem, R., Shinozuka, M.: Structural-system identification I: Theory. J. Eng. Mech. **121**(2), 255–264 (1995)
4. Huang, Z.G., Xu, B., Feinstein, Z., Dyke, S.J.: Nonparametric modeling of magnetorheological damper. In: Proceedings of the Tenth International Symposium on Structural Engineering for Young Experts, Changsha, Hunan, China, pp. 1860–1865 (2008)
5. Ibanez, P.: Identification of dynamic parameters of linear and non-linear structural models from experimental data. Nucl. Eng. Des. **25**, 30–41 (1973)
6. Katkhuda, H., Martinez, R., Haldar, A.: Health assessment at local level with unknown input excitation. J. Struct. Eng. **131**(6), 956–965 (2005)
7. Kerschen, G., Golinval, G.C., Hemez, F.M.: Bayesian model screening for the identification of non-linear mechanical structures. J. Vib. Acoust. **83**, 26–37 (2003)
8. Kerschen, G., Worden, K., Vakakis, A.F., Golinval, J.C.: Past, present and future of nonlinear system identification in structural dynamics. Mech. Syst. Signal Process. **20**, 505–592 (2006)
9. Masri, S.F., Caughey, T.K.: A nonparametric identification technique for nonlinear dynamic problems. J. Appl. Mech. **46**, 433–447 (1979)
10. Masri, S.F., Sassi, H., Caughey, T.K.: A nonparametric identification of nearly arbitrary nonlinear systems. J. Appl. Mech. **49**, 619–628 (1982)
11. Masri, S.F., Miller, R.K., Saud, A.F., Caughey, T.K.: Identification of nonlinear vibrating structures; part I: Formulation. J. Appl. Mech. **109**, 918–922 (1987a)
12. Masri, S.F., Miller, R.K., Saud, A.F., Caughey, T.K.: Identification of nonlinear vibrating structures; part II: Application. J. Appl. Mech. **109**, 923–929 (1987b)
13. Masri, S.F., Caffrey, J.P., Caughey, T.K., Smyth, A.W., Chassiakos, A.G.: Identification of the state equation in complex non-linear systems. Int. J. Non-Linear Mech. **39**, 1111–1127 (2004)
14. Masri, S.F., Caffery, J.P., Caughey, T.K., Smyth, A.W., Chassiakos, A.G.: A general data-based approach for developing reduced-order models of non-linear MDOF systems. Nonlinear Dyn. **39**, 95–112 (2005)
15. Masri, S.F., Tasbihgoo, F., Caffery, J.P., Smyth, A.W., Chassiakos, A.G.: Data-based model-free representation of complex hysteretic MDOF systems. Struct. Control Health Monit. **13**, 365–387 (2006)
16. Mohammad, K.S., Worden, K., Tomlinson, G.R.: Direct parameter estimation for linear and nonlinear structures. J. Sound Vib. **152**(3), 471–499 (1992)
17. Tasbihgoo, F., Caffrey, J.P., Masri, S.F.: Development of data-based model-free representation of non-conservative dissipative systems. Int. J. Non-Linear Mech. **42**, 99–117 (2007)
18. Spencer, B.F. Jr, Dyke, S.J., Sain, M.K., Carlson, J.D.: Phenomenological model of a magnetorheological damper. J. Eng. Mech. **123**(3), 230–238 (1997)
19. Stanway, R., Sproston, J.L., Stevens, N.G.: Non-linear modeling of an electro-rheological vibration damper. J. Electrost. **20**, 167–184 (1987)
20. Xu, B., He, J., Zhou, R., Masri, S.F.: Data-based model free hysteresis identification for nonlinear structures. Eng. Sci. **8**(2), 12–19 (2010)
21. Yang, J.N., Huang, H.W., Lin, S.: Sequential non-linear least-square estimation for damage identification of structures. Int. J. Non-Linear Mech. **41**, 124–140 (2006)
22. Yang, J.N., Huang, H.W.: Sequential non-linear least-square estimation for damage identification of structures with unknown input and unknown output. Int. J. Non-Linear Mech. **41**, 789–801 (2007a)
23. Yang, J.N., Pan, S., Lin, S.: Least-square estimation with unknown excitations for damage identification of structures. Eng. Mech. **133**(1), 12–21 (2007b)

24. Yang, Y.X., Ibrahim, S.R.: A nonparametric identification technique for a variety of discrete nonlinear vibrating system. J. Vib. Acoust. Stress Reliab. Des. **107**, 60–66 (1985)
25. Yun, H.B., Masri, S.F., Wolfe, R.W., Benzoni, G.: Data-driven methodologies for change detection in large-scale nonlinear dampers with noisy measurements. J. Sound Vib. **322**, 336–357 (2009)
26. Wang, D., Haldar, A.: Element-level system identification with unknown input. Eng. Mech. **120**(1), 159–176 (1994)
27. Wang, D., Haldar, A.: System identification with limited observations and without input. Eng. Mech. **123**(5), 504–511 (1997)
28. Worden, K., Tomlinson, G.R.: Nonlinearity in Structural Dynamics: Detection, Identification and Modeling. IOP Publishing, Bristol (2001)
29. Wu, Z.S., Xu, B., Harada, T.: Review on structural health monitoring for infrastructure. J. Appl. Mech. **6**, 1043–1054 (2003)
30. Zhou, Q., Qu, W.L.: Two mechanic models for magneto-rheological damper and corresponding test verification. Earthq. Eng. Eng. Vib. **22**(4), 144–150 (2002)